



**UNIVERSITI PUTRA MALAYSIA**

**DEVELOPMENT OF A NEW COMPOSITE ENERGY-ABSORBER  
SYSTEM FOR AIRCRAFT AND HELICOPTER SUB-FLOORS**

**SIAVASH TALEBI TAHER.**

**FK 2005 24**



**DEVELOPMENT OF A NEW COMPOSITE ENERGY-ABSORBER SYSTEM  
FOR AIRCRAFT AND HELICOPTER SUB-FLOORS**

**By**

**SIAVASH TALEBI TAHER**

**Thesis Submitted to the School of Graduate Studies, Universiti Putra Malaysia,  
in Fulfilment of the Requirement for the Degree of Master of Science**

**September 2005**



Abstract of thesis presented to the Senate of Universiti Putra Malaysia in fulfilment of the requirement for the degree of Master of Science

**A NEW COMPOSITE ENERGY-ABSORBER SYSTEM FOR AIRCRAFT AND HELICOPTER SUB-FLOORS**

By

**SIAVASH TALEBI TAHER**

September 2005

Chairman: Elsadig Mahdi Ahmed, PhD

Faculty : Engineering

Considerable research interest has been directed towards the use of composite for crashworthiness applications, because they can be designed to provide impact energy absorption capabilities which are superior to those of metals when compared on weight basis. The use of composite parts in structural and semi-structure applications is becoming more widespread throughout the automotives, aircraft and space vehicles.

In this study, an innovative lightweight composite energy-absorbing keel beam system has been developed to be retrofitted in aircraft and helicopter in order to improve their



crashworthiness performance. The developed system consists of everting stringer and keel beam. The sub floor seat rails were designed as everting stringer to guide and control the failure mechanisms at pre-crush and post crush failure stages of composite keel beam webs and core. Polyurethane foam was employed to fill the core of the beam to eliminate any hypothesis of global buckling. The numerical prediction was obtained using commercially available finite element analysis software. The experimental data are correlated with predictions from finite element model and analytical solution. An acceptable agreement between the experimental and computational results was obtained. For all structures considered classical axial collapse eigen values were computed.

The results showed that the crushing behaviour of the developed system is found to be sensitive to the change in keel beam core cross-section. Laminate sequence has a significant influence on the failure mode types, average crush loads and energy absorption capability of composite keel beam. The desired energy absorbing mechanism revealed that the innovated system can be used for aircraft and helicopter and meet the requirements, together with substantial weight saving.



Abstrak tesis yang dikemukakan kepada Senat Universiti Putra Malaysia  
Sebagai memenuhi keperluan untuk ijazah Master Sains

**SISTEM KOMPOSIT PENYERAPAN TENAGA BARU UNTUK  
SUB-TAPAK KAPALTERBANG DAN HELIKOPTER**

Oleh

**SIAVASH TALEBI TAHER**

September 2005

Pengerusi: Elsadig Mahdi Ahmed, Ph.D.

Fakulti : Kejuruteraan

Banyak kajian telah dijalankan dalam penggunaan komposit untuk kajian 'crashworthiness' kerana komposit boleh direkabentuk untuk kebolehan penyerapan tenaga yang lebih tinggi jika dibandingkan dengan logam berasaskan berat. Penggunaan tiub bulat komposit dalam applikasi struktur dan semi-struktur semakin tersebar dalam industri automotif, pesawat dan kapal angkasa.

Dalam kajian ini, sistem penyerapan tenaga alur lunas ringan yang inovatif telah dihasilkan untuk pemasangan dalam pesawat dan helikopter bertujuan untuk



memperbaiki prestasi 'crashworthiness'. Gelegar, everting membentuk rel duduk sublantai bertujuan untuk membimbing dan mengawal mekanisma kegagalan pada web dan teras alur lunas komposit di tahap kegagalan pra-hancur dan selepas hancur. Polyurethane digunakan untuk membentuk teras alur tersebut agar lengkukan global dapat dihindarkan. Jangkaan numerikal diperolehi melalui perisian unsur terhingga komersil. Korelasi data eksperimen dengan data dari numerikal dan analitik dilakukan dan didapati ada persetujuan antara kedua-dua data eksperimen dan pengkomputeran. Nilai eigen runtuh sepaksi klasikal dikirakan untuk semua struktur yang dipertimbangkan.

Hasil menunjukkan bahawa kelakuan penghancuran sistem yang dibina adalah peka terhadap perubahan keratan rentas teras alur lunas. Susunan lamina memberi kesan terhadap jenis mod kegagalan, beban purata hancur dan kebolehan penyerapan tenaga alur lunas komposit. Mekanisma penyerapan tenaga terhasil membuktikan bahawa system inovatif ini boleh digunakan untuk pesawat dan helikopter serta memenuhi semua keperluan disamping menjimatkan berat.

## ACKNOWLEDGEMENTS

I would like to express my sincere gratitude and deep thanks to my supervisor Dr. El-Sadig Mahdi Ahmed Saad for his kind assistance, support, advice, encouragement and suggestions throughout this work and during the preparation of this thesis.

A particular note of thanks is also given to the Prof. Dr. Fakhrul-Razi Ahmedun for his suggestions and financial support and members of supervisory committee Dr. Ahmad Samsuri Mokhtar and Mrs. Dayang Laila Abg Abdol Majid for their suggestions and constructive criticisms given at different stages of this study.

Finally, I would like to express my indebtedness to my family for their moral and financial support.



I certify that an Examination Committee met on 28<sup>th</sup> September 2005 to conduct the final examination of Siavash Talebi Taher on his Master of Science thesis entitled “Development of a New Composite Energy-Absorber System for Aircraft and Helicopter Sub-Floors” in accordance with Universiti Pertanian Malaysia (Higher Degree) Act 1980 and Universiti Pertanian Malaysia (Higher Degree) Regulations 1981. The Committee recommends that the candidate be awarded the relevant degree. Members of the Examination Committee are as follows:

**Mohd. Ramly Mohd. Ajir, PhD**

Associate Professor  
Faculty of Engineering  
Universiti Putra Malaysia  
(Chairman)

**Abd Rahim Abu Talib, PhD**


Lecturer  
Faculty of Engineering  
Universiti Putra Malaysia  
(Internal Examiner)

**Mohamed Tarmizi Ahmad, PhD**

Lecturer  
Faculty of Engineering  
Universiti Putra Malaysia  
(Internal Examiner)

**Shahrir Abdullah, PhD**

Associate Professor  
Faculty of Engineering  
Universiti Kebangsaan Malaysia  
(External Examiner)



---

**GULAM RUSUL RAHMAT ALI, PhD**

Professor/Deputy Dean  
School of Graduate Studies  
Universiti Putra Malaysia

Date: 25 OCT 2005





This thesis submitted to the Senate of Universiti Putra Malaysia and has been accepted as fulfilment of the requirements for the degree of Master of Science. The members of the Supervisory Committee are as follows:

**Dr. El-Sadig Mahdi Ahmed Saad, PhD**

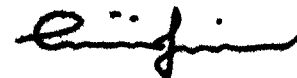
Lecturer  
Faculty of Engineering  
Universiti Putra Malaysia  
(Chairman)

**Dr. Ahmad Samsuri Mokhtar, PhD**

Lecturer  
Faculty of Engineering  
Universiti Putra Malaysia  
(Member)

**Mrs. Dayang Laila Abg Abdol Majid**

Lecturer  
Faculty of Engineering  
Universiti Putra Malaysia  
(Member)



---

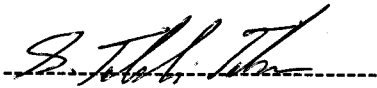
**AINI IDERIS, PhD**  
Professor / Dean  
School of Graduate studies  
Universiti Putra Malaysia

Date: **17 NOV 2005**



## DECLARATION

I hereby declare that the, thesis is based on my original work except for quotations and citations, which have been duly acknowledged. I also declare that it has not been previously or concurrently submitted for any other degree at UPM or other institutions.



SIAVASH TALEBI TAHER

Date: 13/10/2005

# TABLE OF CONTENTS

|   |           |
|---|-----------|
| <b>ABSTRACT</b>   | Page      |
| <b>ABSTRAK</b>  | ii        |
| <b>ACKNOWLEDGEMENTS</b>                                     | iv        |
| <b>APPROVAL</b>   | vi        |
| <b>DECLARATION</b>  | vii       |
| <b>LIST OF TABLES</b>                                       | ix        |
| <b>LIST OF FIGURES</b>                                      | xiii      |
| <b>NOMENCLATURE</b>   | xiv       |
|   | xxii      |
| <b>CHAPTERS</b>   |           |
| <b>1 INTRODUCTION</b>                                       | <b>1</b>  |
| 1.1 Research Objectives                                     | 2         |
| 1.2 Significance of the Study                               | 3         |
| 1.3 Thesis Layout   | 4         |
| <b>2 LITERATURE REVIEW</b>                                  | <b>5</b>  |
| 2.1 Fabric Fibre Reinforced Composites                      | 5         |
| 2.1.1 Glass Fabric Fibre (2D Weaves)                        | 6         |
| 2.1.2 Epoxy Resin   | 8         |
| 2.1.3 Fabrication Processes of Composite Beams              | 9         |
| 2.1.4 Hand Lay-up Fabrication Process                       | 9         |
| 2.2 Energy Absorption Capability of Composite Materials     | 10        |
| 2.2.1 Crashworthiness Parameters                            | 10        |
| 2.2.2 Crushing Behaviour of Composite Materials             | 14        |
| 2.3 Aircraft Sub-structure as Energy Absorption Element     | 20        |
| 2.3.1 Aircraft Crashworthiness                              | 20        |
| 2.3.2 Helicopters   | 22        |
| 2.3.3 Large Airplanes                                       | 24        |
| 2.4 Keel Beam   | 26        |
| 2.4.1 Metallic Keel Beam                                    | 26        |
| 2.4.2 Composite Keel Beam                                   | 28        |
| 2.5 Discussion  | 33        |
| <b>3 EXPERIMENTAL SET-UP</b>                                | <b>34</b> |
| 3.1 Conceptual Design                                       | 36        |
| 3.1.1 Keel Beam Components                                  | 34        |
| 3.1.2 Designed Energy absorption Mechanism of the Keel Beam | 38        |
| 3.2 Experimental Work                                       | 39        |
| 3.2.1 Specimens Types                                       | 42        |
| 3.2.2 Flange (Everting Stringer)                            | 43        |



|          |       |  |            |
|----------|-------|--|------------|
|          | 3.2.3 | Materials  | 45         |
|          | 3.2.4 | Test Procedure   | 45         |
|          | 3.3   | Discussion   | 46         |
| <b>4</b> |       | <b>EXPERIMENTAL WORK</b>                                     | <b>48</b>  |
|          | 4.1   | Keel Beam Type A   | 49         |
|          | 4.1.1 | Load-Displacement Relations                                  | 49         |
|          | 4.1.2 | Energy-Displacement Relations                                | 52         |
|          | 4.1.3 | Crushing History and Failure Modes                           | 55         |
|          | 4.1.4 | Effect of the r/t Ratio on the Load Carrying Capacity        | 61         |
|          | 4.1.5 | Effect of the r/t Ratio on the Energy Absorption Capability  | 62         |
|          | 4.1.6 | Effect of r/t Ratio on the Specific Energy Absorption        | 63         |
|          | 4.2   | Keel Beam Type B   | 65         |
|          | 4.2.1 | Load-Displacement Relations                                  | 65         |
|          | 4.2.2 | Energy-Displacement Relations                                | 68         |
|          | 4.2.3 | Crushing History and Failure Modes                           | 72         |
|          | 4.2.4 | Effect of r/t Ratio on the Load Carrying Capacity            | 78         |
|          | 4.2.5 | Effect of the r/t Ratio on the Energy Absorption Capability  | 79         |
|          | 4.2.6 | Effect of r/t Ratio on the Specific Energy                   | 79         |
|          | 4.3   | Keel Beam Type C   | 82         |
|          | 4.3.1 | Load-Displacement Relations                                  | 82         |
|          | 4.3.2 | Energy-Displacement Relations                                | 86         |
|          | 4.3.3 | Crushing History and Failure Modes                           | 89         |
|          | 4.3.4 | Effect of r/t Ratio on the Load Carrying Capacity            | 95         |
|          | 4.3.5 | Effect of the r/t Ratio on the Energy Absorption Capability  | 96         |
|          | 4.3.6 | Effect of r/t Ratio on the Specific Energy                   | 97         |
|          | 4.4   | Effect of Everting Element on Keel Beam crushing Performance | 99         |
|          | 4.4.1 | Effect of Everting Element on Load-Displacement Relation     | 99         |
|          | 4.4.2 | Effect of Everting Element on Energy-Displacement Relation   | 100        |
|          | 4.5   | Effect of Fibre Sequence on Keel Beam crushing Performance   | 101        |
|          | 4.5.1 | Effect of Fibre Sequence on Load-Displacement Relation       | 10         |
|          | 4.5.2 | Effect of Fibre Sequence on Energy-Displacement Relation     | 104        |
|          | 4.6   | Failure Modes of Keel Beam Composite System                  | 105        |
|          | 4.7   | Conclusion   | 106        |
| <b>5</b> |       | <b>ANALYTICAL SOLUTION AND FINITE ELEMENT SIMULATION</b>     | <b>107</b> |
|          | 5.1   | Analytical Solution  | 107        |



|          |   |            |
|----------|---|------------|
| 5.1.1    | Buckling of Laminated Plates  | 107        |
| 5.1.2    | Buckling of Simply Supported Laminated Plates under In-Plane Load     | 111        |
| 5.1.3    | Analytical Results for Keel Beam                                      | 114        |
| 5.1.4    | Comparison of Experimental and Analytical Results                     | 119        |
| 5.2      | Finite Element work   | 121        |
| 5.2.1    | Modelling Composite Materials Using the ANSYS Finite Element Software | 121        |
| 5.2.2    | Finite Element Model of Keel Beam Edge                                | 124        |
| 5.2.3    | Comparison between Experimental and Finite Element Results            | 132        |
| 5.3      | Conclusion  | 134        |
| <b>6</b> | <b>CONCLUSIONS AND RECOMMENDATIONS</b>                                | <b>135</b> |
| 6.1      | Conclusion  | 135        |
| 6.2      | Recommendations for Future Work                                       | 137        |
|          | <b>REFERENCES</b>   | <b>139</b> |
|          | <b>APPENDICES</b>   | <b>143</b> |
|          | <b>BIODATA OF THE AUTHOR</b>  | <b>159</b> |



## LIST OF TABLES

| <b>Table</b> | <b>Title</b>   | <b>Page</b> |
|--------------|--|-------------|
| 4.1          | Crashworthiness parameters for keel beams with foam ratio FR= 83%. | 64          |
| 4.2          | Crashworthiness parameters for keel beams with foam ratio FR= 56%. | 81          |
| 4.3          | Crashworthiness parameters for keel beams with foam ratio FR= 39%. | 98          |
| 5.1          | Comparison of the experimental and theory eigenvalue analysis      | 119         |
| 5.2          | Comparison between the experimental and FE buckling analyses       | 132         |
| 6.2          | Knock-down factors for the FEM buckling analysis                   | 134         |
| B1           | Test matrix for crush test of Keel beam                            | 157         |



## LIST OF FIGURES

| Figure | Title   | Page |
|--------|---|------|
| 2.1    | Commonly used 2D weave patterns   | 7    |
| 2.2    | Schematic presentation of the load-displacement curve for a composite material under axial crush condition  | 11   |
| 2.3    | Various failures at different scales  | 15   |
| 2.4    | Transverse shearing crushing mode   | 18   |
| 2.5    | Lamina bending crushing mode  | 19   |
| 2.6    | Local Buckling crushing mode  | 20   |
| 2.7    | Mechanism for energy absorption in a helicopter or aircraft. Occupant slowed down by total displacement of gear, sub-floor and seat.  | 22   |
| 2.8    | Front view photos from a high-speed camera showing crash key events of the Sikorsky ACAP helicopter at NASA Langley Research Centre.  | 23   |
| 2.9    | Crash tests of the large transport aircraft (a): Fuselage in drop test rig. (b): Fuselage after drop test. (c) A complete fuselage after crash test   | 25   |
| 2.10   | Typical framework structure of aircraft sub-floor   | 26   |
| 2.11   | Typical framework metallic structure of aircraft sub-floor. (a): Before crash test. (b): After crash test.  | 27   |
| 2.12   | Sine-wave beam concept for energy absorption  | 29   |
| 2.13   | Carbon/Aramid hybrid Energy absorption sine wave beam in Tiger helicopter (Euro copter Company). (a): Tiger internal structures.(b): EA sine wave beam.   | 29   |
| 2.14   | Composite sub-floor and details of the lower forward fuselage. (a): Post test photograph of the sub-floor consisting of two horizontal C-channels, one above the other, with beaded (or waffle) web geometry. (b): Schematic of the lower forward fuselage. | 31   |
| 2.15   | Lear Fan full composite aircraft. (a): Lear Fan prototype in dynamic crash test rig. (b): keel beams in sub-floor. (c) Keel beam specimen after quasi static crushing test.   | 32   |

|     |  |    |
|-----|--|----|
| 3.1 | Schematic representation of the main steps used in the fabrication of the keel beams.  | 36 |
| 3.2 | Beams are assembled in to a sub-floor.   | 37 |
| 3.3 | Final assembling of keel beams in the fuselage   | 38 |
| 3.4 | schematic representation of keel beam crushing mechanism   | 39 |
| 3.5 | stages of keel beam web crushing   | 41 |
| 3.6 | Flow chart describes the experimental work   | 42 |
| 3.7 | General configurations of specimens with foam ratios 39%, 56% and 83%  | 44 |
| 3.8 | Flanges and supports. (a): Plate and flanges assembly and positions of fixing everting flanges. (b): Plate part details. (c): Everting flange details.   | 46 |
| 3.9 | Fabrication stages. (a): Cutting and sizing of composite laminates. (b): Bounding one side of foam. (c): Bounding another side of foam. (d): bounding the sandwich panel on a plywood base. (e): Some final specimens. | 47 |
| 4.1 | Load-displacement curves for three similar keel beam specimens with $r/t=12.5$   | 50 |
| 4.2 | Load-displacement curves for three similar keel beam specimens with $r/t=8.33$   | 51 |
| 4.3 | Load-displacement curves for three similar keel beam specimens with $r/t=6.25$   | 52 |
| 4.4 | Energy-displacement curves for three similar keel beam specimens with $r/t=12.5$   | 53 |
| 4.5 | Energy-displacement curves for three similar keel beam specimens with $r/t=8.33$   | 54 |
| 4.6 | Energy-displacement curves for three similar keel beam specimens with $r/t=6.25$   | 55 |
| 4.7 | The beginning of keel beam crushing.   | 56 |
| 4.8 | Post-buckling failure of web edge immediately after first edge buckling  | 57 |
| 4.9 | Load-displacement curve during pre-crush stage and decreasing the load   | 57 |





|      |  |    |
|------|--|----|
|      | in beginning of post-crush stage   |    |
| 4.10 | First and second buckling failures and a portion of web in threshold of buckling     | 58 |
| 4.11 | Alternative stiffening and softening during buckling of composite web of keel beam   | 58 |
| 4.12 | Buckling in left side web of beam. Crests and node of buckling wave are recognizable | 59 |
| 4.13 | Sequences of failure of keel beam on load-displacement curve                         | 60 |
| 4.14 | Post buckling failure in the both webs of the keel beam                              | 60 |
| 4.15 | Average crushing load as a function of $r/t$ ratio for foam ratio of 83%             | 61 |
| 4.16 | Energy per unit length absorbed as a function of $r/t$ ratio for foam ratio of 83%   | 62 |
| 4.17 | Specific energy as a function of $r/t$ ratio for foam ratio of 83%                   | 63 |
| 4.18 | Load-displacement curves for three similar keel beam specimens with $r/t= 2.5$       | 66 |
| 4.19 | Load-displacement curves for three similar keel beam specimens with $r/t= 8.33$      | 67 |
| 4.20 | Load-displacement curves for three similar keel beam specimens with $r/t= 6.25$      | 68 |
| 4.21 | Energy-displacement curves for three similar keel beam specimens with $r/t=12.5$     | 69 |
| 4.22 | Energy-displacement curves for three similar keel beam specimens with $r/t= 8.33$    | 70 |
| 4.23 | Energy-displacement curves for three similar keel beam specimens with $r/t= 6.25$    | 71 |
| 4.24 | Edge buckling and webs local buckling at the beginning of keel beam crushing.        | 72 |

|      |   |    |
|------|---|----|
| 4.25 | Post buckling failure of edge and web immediately after pre-crush stage                                 | 73 |
| 4.26 | Load-displacement curve during pre-crush stage and decreasing the load in beginning of post-crush stage | 74 |
| 4.27 | Alternative stiffening and softening during buckling of composite web of keel beam                      | 75 |
| 4.28 | Global buckling of keel beam after first edge buckling  | 76 |
| 4.29 | Buckling in left side web of beam. Crests and node of buckling wave are recognizable                    | 76 |
| 4.30 | Post buckling failure in the both webs of the keel beam   | 77 |
| 4.31 | Sequences of failure of keel beam on load-displacement curve  | 77 |
| 4.32 | Average crushing load as a function of r/t ratio for foam ratio of 56%                                  | 78 |
| 4.33 | Energy per unit length absorbed as a function of r/t ratio for foam ratio of 56%                        | 80 |
| 4.34 | energy as a function of r/t ratio for foam ratio of 56%.  | 80 |
| 4.35 | Load-displacement curves for three similar keel beam specimens with r/t= 12.5                           | 83 |
| 4.36 | Load-displacement curves for three similar keel beam specimens with r/t= 8.33                           | 84 |
| 4.37 | Load-displacement curves for three similar keel beam specimens with r/t= 6.25                           | 85 |
| 4.38 | Energy-displacement curves for three similar keel beam specimens with r/t= 12.5                         | 87 |
| 4.39 | Energy-displacement curves for three similar keel beam specimens with r/t= 8.33                         | 88 |

|      |   |     |
|------|---|-----|
| 4.40 | Energy-displacement curves for three similar keel beam specimens with $r/t= 6.25$   | 88  |
| 4.41 | Edge buckling at the beginning of keel beam crushing. In pre-crush stage, edge of beam web, buckles inside the groove of stringer | 89  |
| 4.42 | Post buckling failure of edge and beginning second edge buckling after pre-crush stage  | 90  |
| 4.43 | Load-displacement curve during first edge buckling (pre-crush stage) and second alternating buckling after pre-crush stage        | 91  |
| 4.44 | Alternating load in post-crush stage includes a rising trend and a constant trend region  | 92  |
| 4.45 | Global buckling of keel beam after first edge buckling  | 93  |
| 4.46 | Buckling in left side web of beam. Crests and node of buckling wave are recognizable  | 94  |
| 4.47 | Post buckling failure in the both webs of the keel beam   | 94  |
| 4.48 | Sequences of failure of keel beam on load-displacement curve  | 95  |
| 4.49 | Average crushing load as a function of the $r/t$ ratio for foam ratio of 39%  | 96  |
| 4.50 | Energy per unit length absorbed as a function of the $r/t$ ratio for foam ratio of 39%  | 97  |
| 4.51 | Specific energy as a function of the $r/t$ ratio for foam ratio of 39%  | 98  |
| 4.52 | Load-displacement curves for keel beam specimens with and without everting element  | 100 |
| 4.53 | Energy-displacement curves for keel beam specimens with and without everting element  | 101 |



|      |  |     |
|------|--|-----|
| 4.54 | Load-displacement curves for keel beam specimens with two different lay up for keel beam web                                     | 103 |
| 4.55 | Energy-displacement curves for keel beam specimens with and without everting element   | 104 |
| 5.1  | Edge buckling of keel beam in pre-crush stage  | 108 |
| 5.2  | Simply supported laminated rectangular plate under uniform uniaxial in-plane compression   | 112 |
| 5.3  | Laminate nomenclature  | 115 |
| 5.4  | Buckling loads for a rectangular orthotropic laminated plate in the sequence $[\pm 45]_s$ under uniform compression, $\bar{N}_x$ | 117 |
| 5.5  | Buckling load as a function of the r/t ratio   |     |
| 5.6  | Experimental and analytical initial crushing load as a function of the r/t ratio   | 120 |
| 5.7  | SHELL91 Nonlinear Layered Structural Shell   | 122 |
| 5.8  | Flow chart describes the eigenvalue analysis using the ANSYS finite element program  | 123 |
| 5.9  | Typical Mesh and nodes for keel beam edge composite web  | 124 |
| 5.10 | An eight layer laminate lay-up of the keel beam web in a sequence of $[(\pm 45)_2(0/90)_2]$                                      | 125 |
| 5.11 | General boundary condition for keel beam edge  | 126 |
| 5.12 | Effect of number of mesh on finite element buckling load   | 127 |
| 5.13 | Quadrilateral Shape  | 128 |
| 5.14 | Triangular Shape   | 128 |
| 5.15 | Effect of number of mesh on finite element buckling load   | 128 |
| 5.16 | First four mode of buckling and displacement contour in meter  | 130 |
| 5.17 | First mode shape buckling of finite element model and typical edge buckling of keel beam   | 131 |



|      |   |     |
|------|---|-----|
| 5.18 | The Finite element linear buckling loads for first mode as a function of r/t ratio.   | 131 |
| 5.19 | Experimental and FEM initial crushing load as a function of r/t ratio   | 133 |
| A1   | Core is filled with 83% Polyurethane foam. (a): three view drawing. (b): Sample before test. (c): crushing during test          | 144 |
| A2   | Core is filled with 56% Polyurethane foam. (a): Top and side views drawing. (b): Sample before test. (c): crushing during test  | 145 |
| A3   | Core is filled with 39% Polyurethane foam. (a): Top and side views drawing. (b): Sample before test. (c): crushing during test  | 146 |
| A4   | Trapezoidal filled core with 55% Polyurethane foam. (a): three view drawing. (b): Sample before test. (c): crushing during test | 147 |
| A5   | Triangular foam core keel beam. (a): three view drawing. (b): Specimen in test fixture. (c): crushing during test               | 148 |
| A6   | Multi row zigzag foam core keel beam. (a): three view drawing. (b): Specimen in test fixture. (c): crushing during test         | 149 |
| A7   | Single row zigzag foam core keel beam. (a): three view drawing. (b): Specimen before test. (c): crushing during test            | 150 |
| A8   | C channel composite sandwich ribs core keel beam. (a): Specimen before test. (b): crushing during test                          | 151 |
| A9   | Simple corrugated composite ribs keel beam. (a): Specimen in test fixture. (b): crushing during test                            | 152 |
| A10  | Saw edged corrugated composite ribs keel beam. (a): Specimen in test fixture. (b): crushing during test                         | 153 |
| A11  | Traded edge corrugated composite ribs keel beam. (a): Specimen in test fixture. (b): crushing during test                       | 154 |
| A12  | C-channel composite ribs with parallel cut outs keel beam. (a): Specimen in test fixture. (b): crushing during test             | 155 |
| A13  | Treaded core with 55% Polyurethane foam keel beam. (a): three view drawing. (b): Sample before test. (c): crushing during test. | 156 |



## NOMENCLATURE

| Parameter  | Definition   | Unit                           |
|--|--|--------------------------------|
| a  | Height of plate  | mm                             |
| a/b  | Plate aspect ratio   | mm/mm                          |
| A  | Cross-sectional area   | mm <sup>2</sup>                |
| A <sub>ij</sub>                                  | Elements of extensional stiffness matrix (ij= 1, 2, 6)         | N/m                            |
| b  | Width of plate   | mm                             |
| B <sub>ij</sub>                                  | Elements of coupling stiffness matrix (ij= 1, 2, 6)            | N                              |
| CFE  | Crush force efficiency   | N/N                            |
| C  | Clamp support  |                                |
| C <sub>n</sub>                                   | Clamp support on n <sup>th</sup> side of plate (n=1...4)       |                                |
| c  | Clamp support  |                                |
| D <sub>ij</sub>                                  | Elements of bending stiffness matrix (ij= 1, 2, 6)             | N.m                            |
| δ <sub>p</sub>                                   | Post crush displacement  | mm                             |
| E  | Young's Modulus  | GPa                            |
| E <sub>T</sub>                                   | Total energy absorbed  | kJ                             |
| E <sub>11</sub>                                  | Longitudinal Young's Modulus (direction-1)                     | GPa                            |
| E <sub>22</sub>                                  | Transverse Young's Modulus (direction-2)                       | GPa                            |
| E <sub>s</sub>                                   | Specific energy absorbed                                       | kJ/kg                          |
| ε <sub>x</sub> , ε <sub>y</sub> , ε <sub>z</sub> | Strain in x, y and z directions respectively                   | mm/mm                          |
| FR   | Foam ratio   | m <sup>3</sup> /m <sup>3</sup> |
| F <sub>x</sub> , F <sub>y</sub> , F <sub>z</sub> | Forces in x, y and z directions respectively                   | kN                             |
| G <sub>12</sub>                                  | In-plane Shear Modulus (in the 1-2 Planes)                     | GPa                            |
| H  | Thickness of laminate  | mm                             |
| k <sub>x</sub> , k <sub>y</sub> , k <sub>z</sub> | Curvatures in x, y and z directions respectively               | 1/m                            |
| l  | Length of the part   | mm                             |
| M  | Mass   | kg                             |
| m  | Number of buckle half wavelengths (in x-direction)             |                                |
| M <sub>x</sub> , M <sub>y</sub> , M <sub>z</sub> | Moments resultant in x, y and z directions respectively        | N.m                            |
| M <sub>xy</sub>                                  | Moment resultant in xy-plane                                   | N.m                            |
| n  | Number of buckle half wavelengths (in y-direction)             |                                |
| $\bar{N}_x, \bar{N}_y, \bar{N}_z$                | Stress resultant in x, y and z directions respectively         | N/m                            |
| $\bar{N}_{xy}$                                   | Shear force resultant  | N/m                            |
| P <sub>i</sub>                                   | Initial crushing load  | kN                             |
| $\bar{P}$  | Average crushing load  | kN                             |
| Q <sub>ij</sub>                                  | Elements of reduced stiffnesses matrix (ij=1, 2, 6)            | GPa                            |
| $\bar{Q}_{ij}$                                   | Elements of transformed reduced stiffness matrix (ij= 1, 2, 6) | GPa                            |
| r  | Radius of everting groove                                      | mm                             |
| S  | Simple support   |                                |
| SE   | Stroke efficiency  |                                |
| S <sub>n</sub>                                   | Simple support on n <sup>th</sup> side of plate (n=1...4)      |                                |
| s  | Simple support   |                                |



|            |  |       |
|------------|--|-------|
| $u$        | Displacement (in x-direction)                                | mm    |
| $V$        | Volume   | $m^3$ |
| $v$        | Displacement (in y-direction)                                | mm    |
| $\nu_{12}$ | Poisson's ratio (in the 1-2 Planes)                          |       |
| $V_f$      | Volume fraction of fibre                                     |       |
| $V_r$      | Volume fraction of matrix                                    |       |
| $w$        | Displacement (in z-direction)                                | mm    |
| $W_f$      | Weight of fibre  | kg    |
| $W_m$      | Weight of matrix   | kg    |
| $z_k$      | Distance of $k^{\text{th}}$ layer of laminate from mid-plane | mm    |

# CHAPTER 1

## INTRODUCTION

Structural crashworthiness becomes an essential requirement in the design of automobiles, rail cars and aerospace application. The structural crashworthiness covers the energy absorbing capability of collapsible and non-collapsible elements. The later is designed to provide a protective shell around the occupants i.e. post crash structural integrity.

Traditionally, fuselages of fixed-wing transport aircrafts are made mostly of aluminium [1], a material with a considerable capacity for plastic deformation, hence, an inherent capability to absorb energy in crash situations. Since the last two decades, composite materials are used more extensively to build aircraft structures. However, the crashworthiness aspect related to composite structures has become a serious issue for many space organizations worldwide. For example, NASA Langley Research Center developed an innovative and cost-effective crashworthy fuselage concept for light aircraft and rotorcraft [1, 11].





## **1.1 Composite Keel Beam**

As stated earlier, the primary design goal for crashworthiness is to limit the impact forces transmitted to the occupants. To meet this objective, aircraft or rotorcraft sub-floor elements must be designed for high-energy absorption to prevent structural collapse during a crash [10]. Yet, the sub-floor design must not be so stiff that transmits or amplifies high impact loads to the occupants. Ideally, the design should contain some crushable elements to control limit the loads transmitted to the occupant to survivable or non-injurious levels [2, 10 and 12]. In this case, many investigations have been carried out on sub-floor using crushable elements [4, 5, 13, 14, 15, 16 and 17]. A lightweight energy-absorbing keel beam concept was developed and retrofitted in a general aviation-type aircraft and helicopter to improve crashworthiness performance [4, 13]. For example, more recently in the year 2004 Airbus achieved a world premiere with the A340-600 model, which features the longest carbon fibre keel beam ever built for a civil airliner [18].

## **1.2 Research Objectives**

The primary objective of this current project is to develop a new composite keel beam to be used as main crush element in the aircraft sub floor. Accordingly the detailed objectives are:

1. To design and fabricate everting elements to control composite keel beam